JACS
JOURNAL OF THE AMERICAN CHEMICAL SOCIETY

COMMUNICATION

pubs.acs.org/JACS

Interface Segregating Fluoralkyl-Modified Polymers for High-Fidelity Block Copolymer Nanoimprint Lithography

Vincent S. D. Voet, Teresa E. Pick, Sang-Min Park, Manuel Moritz, Aaron T. Hammack, Jeffrey J. Urban, D. Frank Ogletree, Deirdre L. Olynick,* and Brett A. Helms*

The Molecular Foundry, Lawrence Berkeley National Laboratory, One Cyclotron Road, Berkeley, California 94720, United States

Supporting Information

ABSTRACT: Block copolymer (BCP) lithography is a powerful technique to write periodic arrays of nanoscale features into substrates at exceptionally high densities. In order to place these features at will on substrates, nanoimprint offers a deceptively clear path toward high throughput production: nanoimprint molds are reusable, promote graphoepitaxial alignment of BCP microdomains within their topography, and are efficiently aligned with respect to the substrate using interferometry. Unfortunately, when thin films of BCPs are subjected to thermal nanoimprint, there is an overwhelming degree of adhesion at the mold−polymer interface, which compromises the entire process. Here we report the synthesis of additives to mitigate adhesion based on either PS or PDMS with short, interface-active fluoroalkyl chains. When blended with PS-*b*-PDMS BCPs and subjected to a thermal nanoimprint, fluoroalkyl-modified PS in particular is observed to substantially reduce film adhesion to the mold, resulting in a nearly defect-free nanoimprint. Subsequent lithographic procedures revealed excellent graphoepitaxial alignment of sub-10 nm BCP microdomains, a critical step toward lower-cost, high-throughput nanofabrication.

Block copolymer (BCP) nanolithography is well poised to become a powerful tool for patterning high-density periodic features (typically 10−100 nm) (including arrays, gratings, or other advanced architectures) into a variety of substrates, complementing the ever-growing array of high-resolution nanofabrication techniques.[1] The technology is readily amenable to generating masks, molds, and templates for fabricating components used in micro- and optoelectronics, magnetic storage devices, and nanoporous membranes.[2] The true potential of BCP nanolithography, however, will be realized when the critical dimensions of features reach the single-digit nanometer half-pitch regime (thereby surpassing the resolution afforded by top-down techniques)[3] and when the processes by which features are translated into functional device materials are cost effective.

Toward this end, strongly segregating BCPs such as polystyrene-*block*-polydimethylsiloxane (PS-*b*-PDMS) are nearly ideal materials for obtaining well-ordered, sub-10 nm features via block copolymer lithography. Unfortunately, their implementation has been limited to strategies requiring expensive single-use, top-down methods (e.g., e-beam patterned substrates) to template long-range ordered domains.[4] Recent developments in nanoimprint tools and advanced mold fabrication strategies offer an opportunity to translate templated BCP nanolithography into a high-throughput, cost-effective process.[5] Nevertheless, few examples of nanoimprint lithography (NIL) with BCPs have been demonstrated due to technical challenges which include: (1) difficult mold release from the imprinted film due to high interfacial area and adhesion and (2) nonequilibrium BCP self-assembly within the mold due to poor mobility at interfaces and within confined geometries.[6] Here we report the use of fluoroalkyl-modified homopolymers of either PS or PDMS as mold-release agents when blended with PS-*b*-PDMS during BCP NIL (Figure 1). These polymeric surfactant additives segregate to the BCP−mold interface, which is directed by the fluoroalkyl coating on the mold and the fluoroalkyl group on the homopolymer surfactant. As a result, the low interfacial energy contacts show considerably less adhesion than observed with the BCP alone, and mold release is markedly improved. Concomitantly, the BCP self-assembly is efficiently directed within the mold via graphoepitaxy within one hour of the nanoimprint process. The fidelity of the directed self-assembly of PS-*b*-PDMS and mold release postimprint was readily demonstrated by etching the imprinted film, thereby exposing the PDMS-domains previously encased in the PS matrix. Sub-10 nm features are revealed with this procedure, providing a key advance in BCP NIL toward a high-throughput, robust tool for single-digit nanofabrication.

The synthesis of fluoroalkyl-modified PS (FA-PS) or PDMS (FA-PDMS) proceeded via two distinct routes (Scheme 1). FA-PS was prepared by controlled radical polymerization using a fluoroalkyl-modified alkoxyamine unimer, which was afforded from a well-described hydroxymethyl precursor first reported by Hawker and co-workers.[7] Conversion of **1** to the fluoroalkyl alkoxyamine initiator **3** was accomplished by a modified Mitsunobu reaction using ADDP and PBu_3 with 1*H*,1*H*-perfluorononanol **2** acting as a pseudocarboxylic acid in the transformation. Polymerization of styrene using **3** led to well-defined FA-PS **4** across a broad range of molecular weights with polydispersities less than 1.06 (Figure 2A). FA-PDMS **6** was prepared from **2** using living anionic ring-opening polymerization of 1,1,3,3,5,5-hexamethylcyclotrisiloxane (D3) in the presence of triazabicyclodecene (TBD) as the organocatalyst.[8] Prior to use in BCP NIL, FA-PDMS-OH **5** was capped using trimethylsilylchloride and triethylamine. Several different molecular weights over a range of 3.8−10 kDa were prepared (Figure 2B).

Received: October 19, 2010
Published: February 15, 2011

dx.doi.org/10.1021/ja1094292 | *J. Am. Chem. Soc.* 2011, 133, 2812–2815

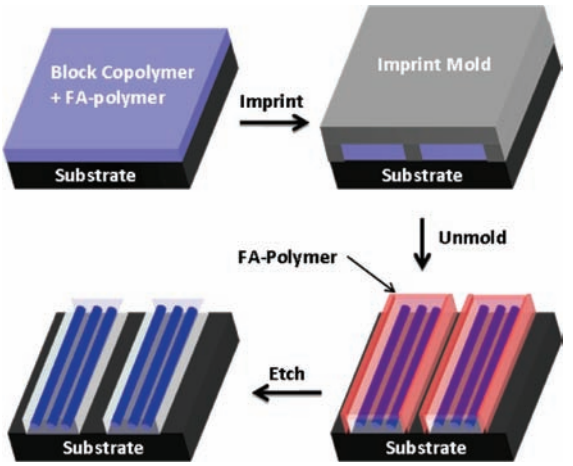

Figure 1. Fluoroalkyl-modified homopolymer (FA-polymer) additives promote mold release and self-assembly in block copolymer thin films during thermal nanoimprint processes. Subsequent lithographic steps reveal underlying equilibrium phase segregated morphologies, which show a high degree of graphoepitaxial alignment with the mold features over the imprinted area.

Scheme 1. Synthesis of Fluoroalkyl-Modified Interface Segregating Polymer Surfactants to Improve Mold Release during BCP NIL: (a) Fluoroalkyl-Polystyrene via Nitroxide-Mediated Controlled Radical Polymerization and (b) Fluoroalkyl-Polydimethylsiloxane via Living Anionic Ring-Opening Polymerization

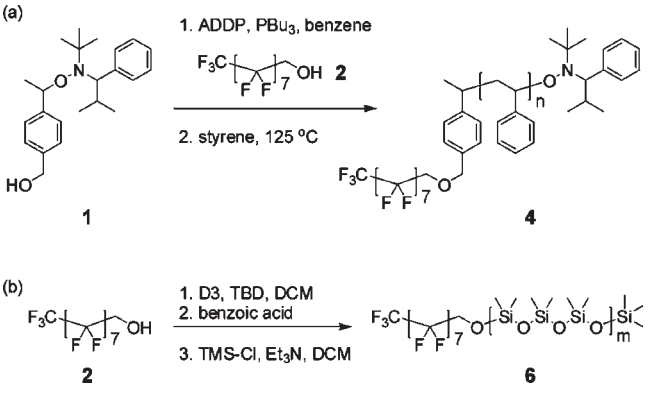

In order to investigate the potential for low interfacial energy fluoroalkyl groups to direct the oriented segregation of FA-PS or FA-PDMS brushes at interfaces, we prepared thin films of these materials or blends thereof and investigated their water contact angles and their surface constituents via XPS. The contact angle of a water droplet on a 35-nm film of PS (M_n = 10 kDa) on a silicon substrate was $\theta_{PS} = 92°$, while that for FA-PS (M_n = 3.2 kDa) was $\theta_{FA\text{-}PS} = 103°$. This deviation reflects the presentation of the lower interfacial energy fluoroalkyl groups toward the polymer−air interface. Water contact angles for PMDS ($\theta_{PDMS} = 103°$) and FA-PDMS ($\theta_{FA\text{-}PDMS} = 105°$) indicated that PDMS and fluoralkyl groups may have similar surface activity. In FA-PS blends (5% w/w) with either a PS homopolymer (M_n = 10 kDa) or a PS-*b*-PDMS ($M_{n,PS}$ = 11 kDa, $M_{n,PDMS}$ = 5 kDa), similar deviations toward larger contact angles than the PS matrix were obtained: $\theta_{FA\text{-}PS+PS} = 100°$ and $\theta_{FA\text{-}PS+PS\text{-}b\text{-}PDMS} = 103°$.

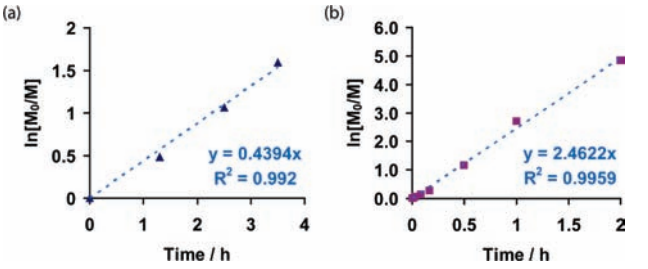

Figure 2. Polymerization kinetics of (a) FA-PS or (b) FA-PDMS. For FA-PS: $[\mathbf{3}]_0$ = 0.11 M; $[\text{styrene}]_0$ = 8.35 M. For FA-PDMS: $[\mathbf{2}]_0$ = $[\text{TBD}]_0$ = 0.040 M; $[\text{D3}]_0$ = 0.80 M. Living polymerizations were demonstrated in both cases.

Contact angle measurements for FA-homopolymers with molecular weights (MWs) in excess of ~3.2−3.8 kDa approached those of their respective homopolymers with increasing MW. Thus, in subsequent work, we employed only the smallest MW FA-PS (M_n = 3.2 kDa) and FA-PDMS (M_n = 3.8 kDa) as these presented the strongest case for segregation to the air−polymer interface.

XPS can be a valuable tool to distinguish surface constituents from the bulk in thin films. In order to determine whether it would be sensitive enough to detect fluoroalkyl-homopolymer surfactant segregation to the air−polymer interface, XPS measurements were carried out on a thermally annealed thin film of FA-PS (M_n = 3.2 kDa, film thickness ~11 nm) deposited onto a silicon substrate modified with a PS brush (Figure S10). For PS, the escape depth of photoelectrons is ~1−2 nm for the 45° glancing angle used here, similar to the radius of gyration for the FA-PS.[9] XPS data were acquired ~1 min after the source was initiated. Fluorine (F) and carbon (C) peaks were observed within the first few minutes, with a F:C ratio of ~0.06. A rapid, exponential decay of this ratio to the noise floor (0.02) was also observed within 5 min, owing to photoelectron-stimulated desorption of fluorinated species during the measurement. Extrapolating back to $t = 0$, the F:C ratio was very close to the expected value of 0.075 for this polymer. The XPS-derived F:C ratio of blends of FA-homopolymers (5% w/w) with either PS-*b*-PDMS or PS did not present above the noise floor. These data suggest that the interfacial segregation of FA-polymer surfactants in blended BCP thin films most likely display submonolayer coverage at the air−polymer interface at this blending ratio and are thus below the detection limit. Nevertheless, as in the case of FA-PS, surface activity directed by the fluoroalkyl chain can already be inferred from contact angle measurements of blended films.

We next sought to determine whether a blend of these fluoroalkyl-modified homopolymers with PS-*b*-PDMS BCPs afforded well-behaved self-assembly in thin films. For our process to be effective, we rely on the fluoroalkyl substituent to induce macrophase separation from the bulk BCP film in favor of their segregation to the air−polymer and mold−polymer interfaces, as driven by the immiscibility of fluoroalkyl substituents with either the PS or PDMS blocks and their lower interfacial energy relative to PS and PDMS. We prepared thin films (32−35 nm) of PS-*b*-PDMS ($M_{n,PS}$ = 11 kDa, $M_{n,PDMS}$ = 5 kDa) blended with 5% w/w of either FA-PS or FA-PDMS. After vacuum annealing the films at 170 °C for 20 h and subsequent cooling, the morphology was revealed after a CF_4/O_2 plasma etching sequence. As shown in Figures 3A, B, the cylinder segregating

dx.doi.org/10.1021/ja1094292 |*J. Am. Chem. Soc.* 2011, 133, 2812–2815

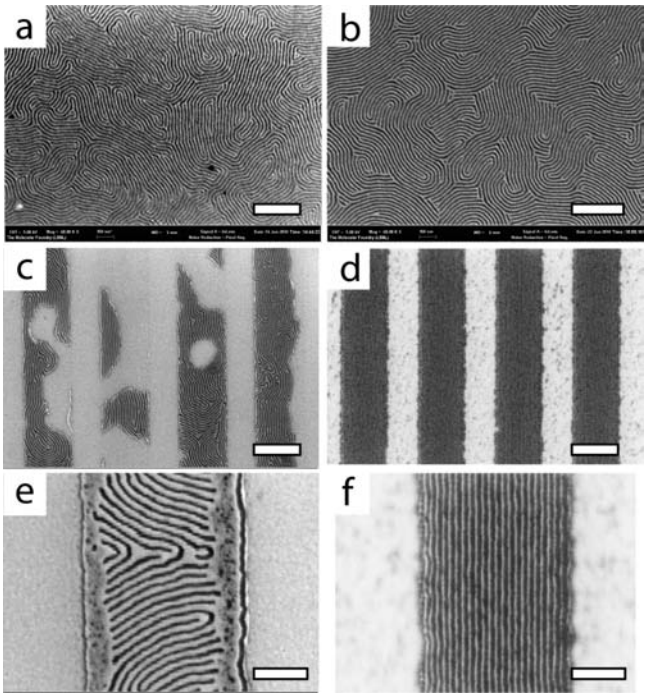

Figure 3. Self-assembly of PS-*b*-PDMS thin films on PS-coated silicon substrates in the presence of (a) FA-PDMS or (b) FA-PS (scale bars represent 300 nm). Directed self-assembly of PS-*b*-PDMS in the presence of (c) FA-PDMS or (d) FA-PS (scale bars represent 600 nm), with magnified images thereof in (e) and (f), respectively (scale bars represent 200 nm).

morphology was readily observed using either fluoroalkyl-modified interface-segregating homopolymer. Morphologies in the blended films were identical to those observed for conventional PS-*b*-PDMS BCP self-assembly in the absence of a fluoroalkyl polymer surfactant. Specifically, a 20-nm pitch was determined in all cases, with the oxidized PDMS features ~8 nm. In addition, the conservation of the domains' sizes indicated that the FA-homopolymers did not blend significantly with the individual PS or PDMS microdomains.

Subsequently, we leveraged the FA-homopolymer surfactant loaded BCP self-assembly process in a thermal nanoimprint scheme for facilitating both mold release and rapid equilibrium microphase separation of the BCP. For these experiments, we prepared a grating mold on a silicon substrate by e-beam lithography. A grating depth of 36 nm with 900 nm pitch (600 nm trench width) was used, thereby ensuring no more than a single layer of cylinders in the imprinted film due to geometrical constraints. The mold was passivated with a fluoroalkyl monolayer using well-described chlorosilane chemistries.[6] Directed self-assembly of BCPs in the presence or absence of FA-homopolymer interface segregating surfactants was investigated during nanoimprint with the mold. Briefly, a solution of PS-*b*-PDMS (1% w/w in toluene) with or without FA-homopolymer (1%, 5%, or 10% w/w with respect to PS-*b*-PDMS) was spin coated onto a silicon substrate modified with a 3-nm-thick PS-brush. The fluoroalkyl-passivated mold was then applied using a hydraulic press (200 psi). To ensure uniform pressure distribution, a rubber compliance layer was added on both sides of the stack. The press was heated at 170 °C for 1 h. After slowly cooling to RT, the mold was carefully released from the substrate. The imprinted substrate was then treated with a CF_4 plasma (10 s, 50 W) followed by an O_2 plasma (13 s, 90 W) to reveal the underlying oxidized PDMS cylinders. Morphologies were analyzed by SEM.

In the absence of our FA-homopolymer additives, significant adhesion of the polymer film to the mold was observed as was poor registration of the BCP self-assembly with respect to the boundaries imposed by trenches in the mold (Figure S13). Similarly poor mold release was observed in the case of FA-PDMS surfactants (Figure 3C). Notably, the domain spacing of the PDMS features increased from L_0 = 20 to 28 nm (Figure 3E). Thus, we concluded that under pressure during the nanoimprint with a fluoroalkyl-passivated mold, there were significant driving forces for the incorporation of FA-PDMS into the PDMS microdomains. While very little BCP residual layer was observed between imprinted features, poor graphoepitaxial alignment was noted, suggesting less mobility of BCPs in their presence within the confined geometry of the mold.

By contrast, FA-PS surfactants gave markedly improved release of the BCP polymer thin film from the mold, with minimal BCP residual layer. Given that the optimum FA-PS loading should depend on surface area and geometry of the mold pattern and associated processing conditions, we tested several FA-PS surfactant loadings. Imprinted BCP thin films at 1% w/w loading FA-PS did not release efficiently, as was found with the parent PS-*b*-PDMS, while at higher concentrations (e.g., 10% w/w) it was difficult to obtain continuous thin films owing to dewetting from the PS-passivated silicon substrate. Notably, a 5% w/w loading of FA-PS with respect to the PS-*b*-PDMS provided continuous films and excellent release post-nanoimprint with no observed changes in the domain spacing within our measurement error (Figures 3 and S15). Graphoepitaxial alignment was significantly improved with FA-PS over FA-PDMS; thus, 8-nm features arising from oxidized PDMS domains were readily observed with excellent long-range ordering as defined by the mold topology (Figure 3, D and F).

Beyond graphoepitaxy as a means to direct BCP alignment in the nanoimprint mold, we also discovered shear flow played an important role. At shorter imprint times (i.e., ~20 min), the BCP microdomains were generally aligned perpendicular to the mold sidewalls as opposed to the parallel orientation expected from graphoexpitaxy (Figure S16). The shear flow near the edges of the trenches, on the other hand, was parallel to the trench long axis. After longer imprint times (i.e., ~1 h), the BCP microdomain alignment was predominantly parallel to the sidewall (i.e., consistent with the thermodynamically most favorable graphoepitaxial alignment), a process likely initiated at the ends of the mold. A full investigation of the kinetics of this process is underway.

The drive toward ever-smaller nanostructures written into substrates for advanced device construction is relentless. To meet the needs of this important endeavor, materials and nanofabrication techniques must converge within the framework of a low-cost, high-throughput scheme. The results presented here demonstrate opportunities to that end brought about by nanoimprint lithography with strongly segregating organic−inorganic block copolymers. By blending our novel fluoroalkyl-polystyrene with PS-*b*-PDMS during self-assembly, we are able to direct BCP self-assembly within the imprint mold while concomitantly establishing a mechanism for improved mold release, due to the interfacial segregation of the fluoroalkyl-modified polymeric surfactant. Thus, for the first time, nearly defect-free long-range ordered sub-10 nm half-pitch features using BCP NIL provides a

significant step toward more robust tools for nanofabrication in this important size regime.

■ ASSOCIATED CONTENT

Supporting Information. Detailed experimental procedures regarding the synthesis, characterization, and application of fluoroalkyl-modified polymers for BCP NIL. Complete reference 5c. This material is available free of charge via the Internet at http://pubs.acs.org.

■ AUTHOR INFORMATION

Corresponding Author
dlolynick@lbl.gov; bahelms@lbl.gov

■ ACKNOWLEDGMENT

Bryan Cord for mold fabrication and Yeon Sik Jung, Xiaogan Liang, and André Kirchner for helpful discussions. All work was performed at the Molecular Foundry and was supported by the Director, Office of Science, Office of Basic Energy Sciences, Division of Materials Sciences and Engineering, of the U.S. Department of Energy under Contract No. DE-AC02-05CH11231.

■ REFERENCES

(1) (a) Bang, J.; Jeong, U.; Ryu, D. Y.; Russell, T. P.; Hawker, C. J. *Adv. Mater.* **2009**, *21*, 4769. (b) Cheng, J. Y.; Ross, C. A.; Smith, H. I.; Thomas, E. L. *Adv. Mater.* **2006**, *18*, 2505. (c) Li, M.; Ober, C. K. *Adv. Polym. Sci.* **2005**, *190*, 183. (d) Gates, B. D.; Xu, Q. B.; Stewart, M.; Ryan, D.; Willson, C. G.; Whitesides, G. M. *Chem. Rev.* **2005**, *105*, 1171. (e) Park, C.; Yoon, J.; Thomas, E. L. *Polymer* **2003**, *44*, 6725. (f) Cheng, J. Y.; Ross, C. A.; Chan, V. Z. H.; Thomas, E. L.; Lammertink, R. G. H.; Vancso, G. J. *Adv. Mater.* **2001**, *13*, 1174. (g) Park, M.; Harrison, C.; Chaikin, P. M.; Register, R. A.; Adamson, D. H. *Science* **1997**, *276*, 1401.

(2) (a) Yang, X. M.; Wan, L.; Xiao, S.; Xu, Y.; Weller, D. K. *ACS Nano* **2009**, *3*, 1844. (b) Jeong, S.-J.; Kim, J. E.; Moon, H.-S.; Kim, B. H.; Kim, S. M.; Kim, J. B.; Kim, S. O. *Nano Lett.* **2009**, *9*, 2300. (c) Stoykovich, M. P.; Kang, H.; Daoulas, K. C.; Liu, G.; Liu, C.-C.; de Pablo, J. J.; Mueller, M.; Nealey, P. F. *ACS Nano* **2007**, *1*, 168. (d) Black, C. T.; Ruiz, R.; Breyta, G.; Cheng, J. Y.; Colburn, M. E.; Guarini, K. W.; Kim, H.-C.; Zhang, Y. *IBM J. Res. Dev.* **2007**, *51*, 605. (e) Guo, L. J. *J. Phys. D: Appl. Phys.* **2004**, *37*, R123. (f) Thurn-Albrecht, T.; Schotter, J.; Kastle, C. A.; Emley, N.; Shibauchi, T.; Krusin-Elbaum, L.; Guarini, K.; Black, C. T.; Tuominen, M. T.; Russell, T. P. *Science* **2000**, *290*, 2126.

(3) (a) Cord, B.; Yang, J.; Duan, H.; Joy, D. C.; Klingfus, J.; Berggren, K. K. *J. Vac. Sci. Technol., B* **2009**, *27*, 2616.(b) *Semiconductor Research Association International Technology Roadmap for Semiconductors*; Semiconductor Research Association: San Jose, CA, 2009; (c) Guo, L. J. *Adv. Mater.* **2007**, *19*, 495.

(4) (a) Yang, J. K. W.; Jung, Y. S.; Chang, J.-B.; Mickiewicz, R. A.; Alexander-Katz, A.; Ross, C. A.; Berggren, K. K. *Nat. Nanotechnol.* **2010**, *5*, 256. (b) Jung, Y. S.; Lee, J. H.; Lee, J. Y.; Ross, C. A. *Nano Lett.* **2010**, *10*, 3722. (c) Ross, C. A.; Jung, Y. S.; Chuang, V. P.; Ilievski, F.; Yang, J. K. W.; Bita, I.; Thomas, E. L.; Smith, H. I.; Berggren, K. K.; Vancso, G. J.; Cheng, J. Y. *J. Vac. Sci. Technol., B* **2008**, *26*, 2489. (d) Jung, Y. S.; Ross, C. A. *Nano Lett.* **2007**, *7*, 2046. (e) Bates, F. S.; Fredrickson, G. H. *Annu. Rev. Phys. Chem.* **1990**, *41*, 525.

(5) (a) Williams, S. S.; Retterer, S.; Lopez, R.; Ruiz, R.; Samulski, E. T.; DeSimone, J. M. *Nano Lett.* **2010**, *10*, 1421. (b) Choi, D. G.; Jeong, J. H.; Sim, Y. S.; Lee, E. S.; Kim, W. S.; Bae, B. S. *Langmuir* **2005**, *21*, 9390. (c) Bailey, T. C.; et al. *Microelectron. Eng.* **2002**, *61*, 461. (d) Dauksher, W. J.; Nordquist, K. J.; Mancini, D. P.; Resnick, D. J.; Baker, J. H.; Hooper, A. E.; Talin, A. A.; Bailey, T. C.; Lemonds, A. M.; Sreenivasan, S. V.; Ekerdt, J. G.; Willson, C. G. *J. Vac. Sci. Technol., B* **2002**, *20*, 2857.

(6) (a) Pina-Hernandez, C.; Guo, L. J.; Fu, P.-F. *ACS Nano* **2010**, *4*, 4776. (b) Honda, K.; Morita, M.; Masunaga, H.; Sasaki, S.; Takata, M.; Takahara, A. *Soft Matter* **2010**, *6*, 870. (c) Alvine, K. J.; Ding, Y.; Douglas, J. F.; Ro, H. W.; Okerberg, B. C.; Karim, A.; Lavery, K. A.; Lin-Gibson, S.; Soles, C. L. *J. Polym. Sci., Part B: Polym. Phys.* **2009**, *47*, 2591. (d) Kim, S.; Lee, J.; Jeon, S.-M.; Lee, H. H.; Char, K.; Sohn, B.-H. *Macromolecules* **2008**, *41*, 3401. (e) Segalman, R. A. *Mater. Sci. Eng., R* **2005**, *R48*, 191. (f) Li, L.; Yokoyama, H. *Adv. Mater.* **2005**, *17*, 1432. (g) Rolland, J. P.; Hagberg, E. C.; Denison, G. M.; Carter, K. R.; DeSimone, J. M. *Angew. Chem., Int. Ed.* **2004**, *43*, 5796. (h) Hong-Wei, Li, H.-W.; Huck, W. T. S. *Nano Lett.* **2004**, *4*, 1633. (i) Deng, T.; Ha, Y.-H.; Cheng, J. Y; Ross, C. A.; Thomas, E. L. *Langmuir* **2002**, *18*, 6719. (j) Segalman, R. A.; Yokoyama, H.; Kramer, E. J. *Adv. Mater.* **2001**, *13*, 1152.

(7) Bosman, A. W.; Vestberg, R.; Heumann, A.; Fréchet, J. M. J.; Hawker, C. J. *J. Am. Chem. Soc.* **2003**, *125*, 715.

(8) Lohmeijer, B. G. G.; Dubois, G.; Leibfarth, F.; Pratt, R. C.; Nederberg, F.; Nelson, A.; Waymouth, R. M.; Wade, C.; Hedrick, J. L. *Org. Lett.* **2006**, *8*, 4683.

(9) Ashley, J. A.; Anderson, V. E. *IEEE Trans. Nucl. Sci.* **1978**, *NS-26*, 1566.